Innovative approach for the application of MTT, LDH and bis-ANS: *ex vivo* modelling of the extracellular beta-amyloid precipitation

PhD Thesis Summary

Emese Szilvia Jánosi-Mózes

Department of Psychiatry
University of Szeged, Faculty of Medicine

Supervisor: Zsolt László Datki, PhD
Doctoral School of Theoretical Medicine

Szeged
2021

Publications the Thesis is based on:

I. **Mozes E**, Hunya A, Toth A, Ayaydin F, Penke B, Datki ZL. A novel application of the fluorescent dye bis-ANS for labeling neurons in acute brain slices. Brain Res Bull. 2011;86(3-4):217-221. doi:10.1016/j.brainresbull.2011.07.004 **IF: 2.818**

II. **Mozes E**, Hunya A, Posa A, Penke B, Datki Z. A novel method for the rapid determination of beta-amyloid toxicity on acute hippocampal slices using MTT and LDH assays. Brain Res Bull. 2012;87(6):521-525. doi:10.1016/j.brainresbull.2012.02.005 **IF: 2.935**

III. Datki Z, Galik-Olah Z, **Janosi-Mozes E**, et al. Alzheimer risk factors age and female sex induce cortical Aβ aggregation by raising extracellular zinc [published online ahead of print, 2020 Jun 9]. Mol Psychiatry. 2020;10.1038/s41380-020-0800-y. doi:10.1038/s41380-020-0800-y **IF: 12.384**

The cumulative impact factor of the publications directly related to Thesis: 18.137

The cumulative impact factor of the whole scientific work: 26.911

ABBREVIATIONS

Aβ, Aβ1-42 → amyloid-beta; **ACSF** → artificial cerebrospinal fluid; **AD** → Alzheimer's disease; **AMPA** → amino-3-hydroxy-5-methyl-4-isoxazolepropionic acid; **ANS** → 8-Anilinonaphthalene-1-sulfonic acid; **APP** → amyloid precursor protein **bis-ANS** → 4,4'-dianilino-1,1'-binaphthyl-5,5'-disulfonic acid, fluorescent probe; **CA1, CA2, CA3** → Cornu Ammonis region of the hippocampus; DG → dentate gyrus (of the Hippocampus); **DiI** → 1,1'-dioctadecyl-3,3,3'3'-tetramethylindocarbocyanine perchlorate, carbocyanin fluorescent dye ; **DiO** → 3-octadecyl-2-[3-(3-octadecyl-2(3H)-benzoxazolylidene)-1-propenyl]-, perchlorate; **DMSO** → dimethyl sulfoxide; **EDTA, CaEDTA** → ethylenediaminetetraacetic acid and its Ca2+-saturated version; **ExViS** → *ex vivo* system; **FBS** → fetal bovine serum; **fEPSP** → field excitatory postsynaptic potentials; **h-Aβ** → human amyloid-beta; **HBS** → HEPES-buffered saline**,** **HEPES** → 4-(2-hydroxyethyl)-1-piperazineethanesulfonic acid; **Hil** → hilus (of the Hippocampus); **Kd** → equilibrium dissociation constant; **LDH** → lactate dehydrogenase; **LTP** →

long-term potentiation; **MAP2** → microtubule-associated protein 2; **MEA** → multi-electrode array; **MTT** → 4,5-dimethylthiazol-2-yl)-2,5-diphenyltetrazolium bromide; **NADPH** → Nicotinamide adenine dinucleotide phosphate; **NFI** → normalized fluorescence intensity; **NMDA** → N-Methyl-D-aspartic acid or N-Methyl-D-aspartate; **OD** → optical density; **OGD** → oxygen-glucose deprivation; **OHSC** → Organotypic hippocampal slice culture; **PI** → propidium iodide; **r-Aβ** → rat amyloid-beta (AβΔ2His); **sAPPα** → soluble amyloid precursor protein (cleaved by alpha-secretase); **SH-SY5Y** → human neuroblastoma cell line; **Sub** → subiculum (of the Hippocampus); **TBS** → theta-burst stimulation; **TPEN** → N,N,N′,N′-tetrakis(2-pyridinylmethyl)-1,2-ethanediamine; **ZnT3** → zinc transporter 3.

1. Introduction

Over the course of Alzheimer's disease (AD), up to 80% of neurons in the hippocampus die, consequently the progressive symptoms of the disease manifest themselves as cognitive disturbances, disorientation and inability to form new memories, specifically those regarding time and location. With its high density of glutamate receptors, in particular N-methyl-D-aspartate (NMDA) receptors, the hippocampus is known to play fundamental role in some forms of learning and memory. The activation of postsynaptic NMDA receptors triggers signal cascades that are crucial for inducing long-term potentiation (LTP) and neuronal plasticity.

Recent improvements in brain slice technology have made *ex vivo* models increasingly useful for studying the pathophysiology of neurodegenerative diseases in a tissue context. While preserving the tissue architecture and synaptic circuitry, the technology also has its advantages compared to *in vivo* models, excluding lengthy animal surgery to model neuropathology of brain injury or laborious monitoring of multiple physiological parameters. Hippocampal slices have been validated to be a capable experimental model for investigating the structural and functional features of synapses at the molecular, cellular, and circuit levels. The key of successful and physiologically relevant measurements performed on acute hippocampal slices is to maintain the tissue viability as long as possible within conditions mimicking the *in vivo* physiological conditions. Our laboratory developed a device, an *Ex Vivo* System (ExViS), that serves as a cost-effective and convenient tool to maintain acute brain tissue viability during several hours lasting treatments.

Beta-amyloid peptide (Aβ) is one of the main protein components of senile plaques associated with AD. Although these plaques may have harmful properties, soluble oligomeric forms of Aβ have been shown to be particurarly

neurotoxic. Measuring the toxic effect of different Aβ aggregation species as well as the neuroprotective effect of novel drug candidates requires a reliable and relevant assay. Along with electrophysiology measurements on *ex vivo* brain slices, 4,5-dimethylthiazol-2-yl)-2,5-diphenyltetrazolium bromide (MTT) , a yellow tetrazole assay has been the most commonly used method for measuring the impact of Aβ toxicity on cell viability in neuronal cell cultures. Our goal was to develop a rapid and reliable test for Aβ toxicity measurement within the tissue context of the hippocampus. We enriched our model with an additional relevant event of the ageing brain: in addition to Aβ1-42 treatment acute slices underwent a mild oxygen-glucose deprivation (OGD) as well. Cerebral hypoperfusion is an early event in AD and increases the risk to develop the disease. Measuring Aβ toxicity on OGD acute hippocampal slices could be a relevant model and an easy *ex vivo* quantitative method to screen protective agents.

We can gain deeper understanding about the investigated neurodegenerative phenomenons in the brain and hippocampus by correlating cellular level physiological analyses with static images obtained within the larger context of the tissue. Aβ oligomerization studies *in vitro* and on acute hippocampal slices executed in our laboratory lead us to the discovery and further exploration of the neuron labelling properties of the oligomer-specific fluorescent dye, 4,4'-dianilino-1,1'-binaphthyl-5,5'-disulfonic acid (bis-ANS). Our study presents a novel application of the bis-ANS for the detection of mechanically damaged neurons on the surface of acute hippocampal slices and its properties are visaulized in the context of the already extensively explored propidium iodide (PI) and 1,1'-dioctadecyl-3,3,3'3'-tetramethylindocarbocyanine perchlorate (DiI) tracers.

Zinc plays crucial role in synaptic plasticity, learning, and memory and numerous studies have suggested that the disruption of its homeostasis, – both depletion and excess – is linked with various neurodegenerative diseases including AD. Zn^{2+} ion released from neurons interacts with Aβ, and is enriched in senile plaques in the brain of AD patients. Secreted Zn^{2+} binds to NMDA, amino-3-hydroxy-5-methyl-4-isoxazolepropionic acid (AMPA) and glycine receptors and it also regulates their dynamics. Zn^{2+} in the hippocampus is essential for the induction of LTP. In our recently published study we showed that after inducing massive Zn^{2+} release on acute hippocampal slices, Aβ1-42 could be rapidly aggregated into bis-ANS reactive species (where bis-ANS was used as an oligomer-specific fluorescent probe). Consequently, LTP and hippocampal viability is attenuated.

2. Aims

During the course of my PhD work, in tight-knit teamwork, I set and completed the following goals:

1. Developing and tailoring novel approaches for the application of MTT and lactate dehidrogenase (LDH) assays on acute hippocampal slices modelling the ageing brain in order to measure the effects of Aβ1-42 aggregation and potential protective agents.
2. Exploring a novel feature and application possibility of bis-ANS fluorophore to label neurite cross-sections and engage in detailed fluorescent imaging of neuronal structures in *ex vivo* hippocampus.
3. *Ex vivo* modelling of Zn^{2+}-induced Aβ aggregation and measuring its effect on viability and synaptic function.

3. Materials and Methods

3.1. Preparation of the acute hippocampal and other brain tissue slices

Following narcosis with chloral hydrate (0.4 g/kg) 10 ± 1-week-old male Wistar rats were decapitated. The heads without scalp-skin were placed in ice cold distilled water for 1 min. The brains were quickly removed and immersed in minimal Ca^{2+}-containing artificial cerebrospinal fluid (ACSF, preparation solution) with elevated Mg^{2+} at 4 ºC. The composition of the preparation solution was the following (in mM): NaCl 127; KCl 2; $MgCl_2$ 3.5; $CaCl_2$ 0.5; $NaHCO_3$ 25; d-glucose 10; pH = 7.4. 0.4 mm thick brain tissue slices were prepared from hippocampus, cerebellum and neocortex using McIlwain tissue chopper at 4 ºC. The surface area of the slices was determined with a preparation microscope directly after preparation. The well area (15 mm^2) was used for area calibration. The slices (area ≈9 mm^2) were rapidly transferred into a mini-chamber for further treatment or into Petri dishes for labelling.

3.2. H-ACSF solutions required in different experiments

The following 4-(2-hydroxyethyl)-1-piperazineethanesulfonic acid (HEPES)-containing ACSF solutions were used in the experiments (concentrations are given in mM):

- H-ACSF/1: NaCl 122; KCl 3; $CaCl_2$ 0.3; $MgCl_2$ 3.7; $NaHCO_3$ 25; HEPES 5; d-glucose 10; pH=7.4.
- H-ACSF/2: NaCl 132; KCl 3; $CaCl_2$ 2; $MgCl_2$ 2; $NaHCO_3$ 25; HEPES 5; pH=7.4.

- H-ACSF/3: NaCl 120; KCl 3; $CaCl_2$ 2; $MgCl_2$ 2; $NaHCO_3$ 25; HEPES 5; d-glucose 12; pH=7.4 (with normal calcium, magnesium and glucose levels).

3.3. Fluorescent labelling of acute hippocampal slices

From the tissue chopper's plate, brain slices were rapidly transferred into Petri dishes for labelling. After rewashing, hippocampus slices were transferred to a cover slip mounted glass slide. In every case we controlled the distance between two glasses with an adhesive-paper (thickness 0.4 mm). As a result, all anatomically undamaged hippocampus slices from the median part (± 2 mm from middle) of the hippocampus were suitable for the experiments.

The labelling solution was composed of the following (in mM): NaCl 129; HEPES 20; $NaHCO_3$ 10; sucrose 10 (pH = 7.4), supplemented with 10 M bis-ANS, 3 μM PI or 50 μM DiI (in 1% dimethyl sulfoxide [DMSO] solution).

Bis-ANS and PI were applied simultaneously for 10 min, while in bis-ANS/DiI co-staining experiments the two dyes were applied consecutively. First, treatment with DiI for 15 min and after washing with the labeling solution described above, Bis-ANS was applied for 10 min.

3.4. Neuroblastoma *in vitro* cell culturing and fluorescent labelling

SH-SY5Y cells were plated for 24 h at 37 ºC in Petri dishes at a density of 3×104 cells per well to 5% confluency. CO_2 in a humidified atmosphere with Dulbecco's Modified Eagle's Medium (MEM):F-12 (1:1) with phenol red. l-Glutamine (4 mM), penicillin (200 units/ml), streptomycin (200 g/ml), MEM non-essential amino acid solution (100× liquid mg/L) and 10% fetal bovine serum (FBS) were added to the medium. After mechanically damaging the cells by cutting a straight line on the Petri dish surface with a blade they were incubated in the presence of bis-ANS (10 μM) and PI (3 μM) for 10 min.

3.5. Fluorescence microscopy

Measurements were performed at room temperature (24 ºC). Images were taken with a 24-bit digital Colour-View II FW camera (with CCD arrays of 2080 × 1544 pixels) interlocked with the imaging system of an OLYMPUS IX71 inverted research fluorescence microscope. Image acquisition and analysis were performed by analySIS 3.2 software. To detect the fluorescence of the dyes we used the following wavelengths (ex./em.): 380/535 nm (bis-ANS), 530/620 nm (PI) and 550/620 nm (DiI).

3.6. Aβ1-42 treatment of hippocampal slices

After the preparation of the slices in ice cold H-ACSF/1 solution photos were made of them for measuring the slice area. Slices (with an area of

approximately 9 mm2) were quickly transferred into a mini-chamber (max. 5 slices in 1 ml H-ACSF/1) for conditioning (30 min) in the carboxygenated (95/5% : O_2/CO_2) preparation solution at room temperature (24 ºC).

After 30 minutes hippocampus slices were transferred from the mini-chamber into the plastic Petri dish and was left to rest at room temperature in glucose- and carboxygen-free H-ACSF/2 (3 mL/Petri dish) for one hour. (The Petri dish was continuously being stirred at 370 rpm by a modified BIOSAN TS-100 thermo shaker). After one hour oxygen-glucose deprivation the supernatant (H-ACSF/2) in the Petri dish was changed to H-ACSF/3 solution (3 mL/Petri dish). The slices were quickly transferred into the mini-chambers (maximum 5 slices in 1 mL) for treating them with freshly prepared oligomeric Aβ1-42 peptide adding 50 µL stock solution of the peptide into 950 µL H-ACSF/3 in each chamber (final concentration of Aβ1-42: 20 µM). Foaming was inhibited by a floating plastic ball (diameter: 5 mm) applied in the mini tube chambers. Classic apoptotic factors (e.g. NaN_3, H_2O_2, KCN and Thapsigargin) were used as controls in these experiments.

3.7. MTT and LDH measurements

After treating the slices with 20 µM Aβ 1-42 for 4 hours, the supernatant (to be used in LDH assay) was changed to H-ASCF/3 (0.9 mL/chamber) and 0.1 mL MTT stock solution (5 mg/mL H-ACSF/3) was added (MTT final concentration: 0.5 mg/ml). The chamber was left to rest for 15 min without carboxygenation. To stop further reduction of MTT, the medium (H-ACSF/3) was removed. Then pure DMSO (100 µL/slice/well) was added for dissolving formazane from the slices. (30 min in a 96-well plate). Then 70 µL DMSO solution from each slice (well) was transferred into another 96-well plate. The optical density (OD) of the dissolved formazane was measured at 550 and 620 nm. The following formula was used for synchronizing the data: (OD550 – OD620)/area of slice (mm^2) = 100% in control (Aβ1-42 untreated slices).

For LDH measurements the above mentioned supernatants (H-ACSF/3) of the 4 hours Aβ1-42 treament of slices were used. Supernatants were centrifuged at 500 x *g* for 10 min and the LDH activity was measured with a standard LDH kit. The results were calculated with the following formula: (OD450 – OD620)/mean area of slices (mm^2) = 100% in control (Aβ1-42 untreated chamber).

3.8. *Ex vivo* fluorescent detection of the vesicular Zn^{2+} release and Zn^{2+}-induced Aβ oligomerization

The kinetics of the change in the fluorescence intensity was measured with a 96-well plate specific NOVOstar OPTIMA plate reader using fiberglass (Ø 3

mm, 20 flashes/well/cycle) optics that allowed the detection of the total area of the slice in a well.

After resting for 30 minutes in the mini-chamber system (described in Chapter 4.1) at room temperature in Ca^{2+}-free, carbogenated ACSF solution, the slices (maximum 10) were washed for 30 secs in 2 mL preheated (36 ºC) HEPES buffered saline (HBS, composition in mM: NaCl 125; KCl 2; $CaCl_2$ 2; $MgCl_2$ 2; HEPES 25; d-glucose 12; at pH=7.4. and 36 ºC). Next, brain slices were transferred from the mini-chamber into the plate wells (bottom area: 15 mm^2) using pipettes (type 20-200 µL) that were cut-off at their tip. Slices were transferred together with their media: 120 µL HBS per well. HBS solution was removed very carefully from the slices with a pipette and was replaced with

a) RhodZin3, a Zn^{2+}-specific fluorescent dye diluted in HBS solution (10µM, 40 µL per well) in order to monitor endogenous zinc release; or

b) Bis-ANS, as Aβ oligomer specific fluorophore in 10 µM concentration to monitor Aβ-Zn^{2+} aggregation. Consequently, in the Zn-Aβ precipitation measurements the Bis-ANS-HBS solution was supplemented with synthetic human or rat Aβ peptide (50 µM). Before each assay the stock solution of Aβ peptide (0.5 mM) was freshly preparated in distilled water (pH=5).

Each well accommodated one immobilized slice in central position. Immobilization was achieved by a round plastic web with 40 µm pore diameter, with no autofluorescence and handled with ceramic forceps. This process ideally took up a maximum of 2 minutes per 10 slices. The plates and the HBS solution were preheated at 35-36 ºC before slices were put into them. The temperature inside the plate-reader was also 36 ºC. The distance between the plastic web (which is placed on the slice) and the top of the well was consistently 9 mm (we checked the distance at each measurement with the help of a plastic tube, which was marked at 8.9 mm).

For KCl treatment (final concentration 50 mM) we took advantage of the built-in liquid micro-pipettor (minimal pipetting capacity is 1 µL) in the plate reader with an injection speed of 420 µL/sec. Fluorescence intensity tracking begun 1 min before the treatment of slices with KCl. *Ex vivo* Zn^{2+} release and precipitation with Aβ fluorescent tracking required high slice viability (in HBS solution) only for the period of the KCl-induced massive depolarization and intensive vesicular Zn^{2+} release (maximum 3 min), since after the Zn^{2+} was released into the extracellular space, the detected reactions (Zn-dye or Aβ-dye complexes) were rather chemical than physiological. The normalized fluorescence intensity (NFI) in the Zn^{2+} release and Zn-Aβ precipitation measurements were calculated via the following formula: $[(Fmax-F^0)/F^0]$/area of slice (mm^2), where F^0 is the initial fluorescence intensity of the dyes in the measurements before treatments. F_{max} is the maximum amplitude of the

fluorescence intensity caused by Zn^{2+}-release. Maximum 10 wells (one slice per well) can be scanned in one cycle (RhodZin3 λ ex. 550, em. 580 nm; bis-ANS: λ ex. 350 nm, em. 540 nm).

One cycle took 10 sec (the scanning of each well in a cycle lasted for 1s with 20 flashes). We detected the Zn^{2+} specificity, concerning vesicular Zn^{2+} release, by adding CaEDTA. To survey Zn^{2+} specificity, only CaEDTA could be used in Zn-Aβ precipitation measurements. The heading of excitation and emission light in the fiberglass optics was retrograde. We used the well-bottom-detection form in our measurements.

3.9. Multi-electrode array (MEA) electrophysiology

One acute hippocampal slice was placed in a 3D-MEA chip with 60 tip-shaped and 60-μm-high electrodes spaced by 100 μm. The surrounding solution was removed, and the slice was immobilized by a grid. The slice was continuously perfused with carbogenated ACSF (1.5 mL/min at 34 °C) during the whole recording session. Prior to an experiment, slices were washed twice with ACSF, and then incubated (± CaEDTA 0.1 mM to reverse the Zn^{2+}-induced Aβ aggregates) for a further 1 h in the incubation chamber, to ensure that that the preparation was not affected by residual K^+ or peptide remaining in the media. The slices were then stabilized for 30 min on the MEA chip.

Data were recorded with a Multi Channel System. The Schaffer-collateral was stimulated by injecting a biphasic current waveform (100 + 100 μs) through one selected electrode at 0.033 Hz. We took care to choose the stimulating electrode in the same region from one slice to the other. The peak-to-peak amplitudes of field excitatory postsynaptic potentials (fEPSPs) at the proximal stratum radiatum of CA1 were analyzed. Following a 30 min incubation period, slices were continuously stimulated with medium-strength stimuli. When stable evoked fEPSPs were detected (for at least 20 min), the stimulus threshold was determined, and a stimulus strength–evoked response curve (i.e. input–output, I–O curve) was recorded by gradually increasing stimulus intensity until the maximal stimulus strength was reached. The I–O curve for each slice did not show any significant differences between the treatment groups, indicating normal basal synaptic function. The stimulus intensity was continuously increased from 0 to 120 μA with 10 μA steps. Stronger stimulation led to large Faradic effects on the electrodes causing artifacts data sets were recorded for each stimulation intensity. The intensity of the test stimulus was set to be 30% of the threshold and maximum stimulus strength interval. After recording a 10 min stable control sequence, LTP was induced by applying theta-burst stimulation (TBS; trains of 15×100 Hz bursts, 5 pulses per burst with a 200 ms interburst interval), at the maximum stimulation intensity, then fEPSPs were recorded for 60 min.

3.10. Statistical analysis

Data are presented as means ± standard error of mean (S.E.M). Student-t test and ANOVA *post hoc* test Bonferroni was used for statistical evaluation using Microsoft Excel and SPSS 10.0 for Windows software. The differences were compared with the control measurements of each conditions. The values were considered statistically significant at the level $p \leq 0.001$ and $p \leq 0.05$, unless otherwise stated in figure legends.

4. Results

4.1. Experiments on acute hippocampal slice viablity and amyloid-beta toxicity

4.1.1 Solving the acute brain tissue survival at several hours lasting treatments with *ExViS* proprietary system

The treatment and toxicity measurements on acute, *ex vivo* hippocampal slices, described below require approx. 4-6 hours of tissue survival. To keep the acute features of the hippocampus tissue, we placed the slices into a specific carbogenating (5% CO_2, 95% O_2) system, designed in our laboratory (*ExViS*). A rounded bottom chamber with a 1 mL working volume is the crucial part of the proprietary system. The treatment and/or the carbogenation of the tissue slices can take place in room or body (36 ºC) temperature in this semi-hermetically closed chamber by a threaded plug with a rubber sealing. This plug serves as a manual precision control of tthe carbogene gas pressure. A needle (Ø=0.6mm) vertically goes through the plug connected to a rigid plastic tube outside the chamber, upon which there is a regulation valve for the gas current. The more slices get into the chamber, the shorter the time they can be stored in their vital form in the same volume. Up to 10 slices can be treated or incubated safely at the same time and in the same chamber for 30 min. However, in our subsequently developed similar method described later in this thesis, where acute hippocampal slices had been used to determine Aβ toxicity with MTT and LDH assays, the treatment and viability was maintained for 4 hours (5 slices/1 mL).

4.1.2 Validation of *ExViS*

ExViS system has been validated via MTT viability assay and electrophysiology.

MTT Assay Results: After 30 and 180 min resting or treating in carbogenated standard ACSF solution (36 ºC) we found no significant difference in the mitochondrial reduction capacity of the acute slices, while the viability of the non-carbogenated hippocampal slices (under 180 min) decreased significantly.

Electrophysiology Results: TBS-induced LTP was recorded to determine whether any alterations in synaptic transmission between neurons occur during the incubation/treatment time. Field EPSPs were recorded from the distal and proximal part of the stratum radiatum in hippocampal CA1. The increase of fEPSP amplitude was persistent in both regions 60 min after TBS.

4.1.3 Measuring Aβ1-42 toxicity on glucose-oxygen deprived hippocampal slices with MTT and LDH assay

The workflow of the developed protocol is outlined in the following steps:

1. After removing from the brain and preparation, hippocampal slices were left to rest for 30 min in carbogenated H-ACSF/1 at 24 ºC for conditioning.
2. Next, mild OGD was applied for 1 h in H-ACSF/2 solution in Petri dish.
3. Treatment of the slices in the mini-chamber with oligomeric Aβ1-42 peptide for 4 hours in H-ACSF/3 solution.
4. Slice viability was measured with MTT and LDH assays.

The concomitant use of the two assays in acute, OGD hippocampal model provided coherent results on the toxic effect of Aβ1-42. The results of both MTT and LDH assays show that one-hour resting under mild OGD reduces brain tissue viability. Simultaneous treatment of slices with OGD and oligomeric Aβ1-42 induced the most intensive decrease in hippocampal slice viability.

4.2. A novel aplication of the fluorescent dye, bis-ANS, labelling neurons in acute brain tissue

In our experiments described later in the following chapter we used the non-covalent extrinsic fluorophore bis-ANS to explore the relationship between Zn^{2+} and Aβ1-42. As a result of an accidental event, we observed that the dye is suitable to label the tissues of acute hippocampal slices along with neuronal structures in dentate gyrus (DG), Cornu Ammonis (CA) 1–3 regions, hilus (Hil) and subiculum (Sub).

Our findings about the newly discovered neuron-labelling properties of bis-ANS were the following:

1. **bis-ANS only labels live tissue.** Formaldehyde-fixed hippocampal slices emitted non-specific homogenous fluorescence in contrast to the acute, live slices.
2. **In the $NaHCO_3$-free (only HEPES-buffered) solution no specific bis-ANS signals could be detected** after 10 min of staining. It

appears that the fluorescence emission of bis-ANS is $NaHCO_3$-dependent, although the mechanism is unknown.

3. **bis-ANS only labels membrane-damaged cells.** An incision was made by the dint of a blade on the non-differentiated SH-SY5Y human neuroblastoma monolayer cell culture settled in the Petri dish. After 10 min of staining with bis-ANS and PI (labels the nucleus of mechanically damaged cells) we analyzed the samples using fluorescence microscopy and co-localized the digital images. Only the cells that were situated by the incision absorbed the dyes.

4.3. Effects of Zn^{2+}-induced Aβ toxic aggregation cell viability and synaptic function

4.3.1 K^+-induced Zn^{2+} release in different *ex vivo* brain tissue slices

KCl (50 mM) treatment causes massive depolarization in neurons and induces Zn^{2+} release into the media. The intensity of Zn^{2+} release in slices originating from different brain areas was measured using a Zn^{2+}-specific fluorescent dye, RhodZin3. The characteristic fluorescence kinetics of the thalamical, neocortical and hippocampal slices significantly differed from each other and the greatest fluorescence intensity was produced by the hippocampal slices. This finding is consistent with current literature. The cortical slices alsoemitted meaningful signal but at smaller magnitude compared to hippocampal slices. Thalamic samples did not show detectable Zn^{2+} release, as it was also expected based on previous findings.

4.3.2 Zn^{2+}-induced Aβ aggregartion *in vitro*

We characterized Aβ aggregation in response to Zn^{2+} in cell-free system. Aggregation was monitored with bis-ANS, the fluorophore originally designed to detect peptide aggregation into pre-fibrillar, low-order oligomers. We found that Zn^{2+} (50 μM) triggered significant aggregation of human Aβ1-42 (50 μM) within seconds, which then was rapidly reversed by adding the Zn^{2+}-selective chelator, CaEDTA (0.5 mM) into the media. In the absence of Zn^{2+}, human Aβ1-42 aggregated relatively slowly and incompletely and was not influenced by KCl (50 mM), the compound used in our next experiments to stimulate Zn^{2+} release in acute brain slices from rat.

4.3.3 K^+-induced Zn^{2+} release affects Aβ aggregation on *ex vivo* acute hippocampal slices

Human Aβ1-42 could be rapidly aggregated into bis-ANS reactive species by endogenous hippocampal Zn^{2+} released upon the stimulation with K^+. Rapid Aβ1-42 aggregation from the slices was inhibited when Ca^{2+} was deleted from the high K^+ buffer, consistent with the fact that the aggregating factor is being released upon synaptic activation. Aggregation could be reversed by the zinc-

selective chelator, CaEDTA, and no aggregation was observed with high K^+ treatment of slices in the presence of AβΔ2His (rat-Aβ), consistent with the aggregating factor being Zn^{2+} released by the hippocampus upon depolarization.

4.3.4 *Ex vivo* Zn^{2+} and Aβ treatment of acute hippocampal slices

4.3.4.1 Toxic effect of Zn^{2+} and Aβ treatment

To determine whether the toxicity of Aβ1-42 could be induced by Zn^{2+}, we performed MTT viability assay on hippocampal slices treated with Aβ and Zn^{2+} (both 15 μM). The slices had not been exposed to high K^+. MTT assay results indicated that, after 3-hour treatment neither Zn^{2+} nor Aβ alone inhibited viability, but when added together, Aβ1-42 and Zn^{2+} effect was markedly toxic ($p<0.001$). There was no loss of viability following a 3-hour control incubation.

4.3.4.2 LTP impairment after co-treatment with Zn^{2+} and Aβ

Zn^{2+} treated slices displayed significantly smaller responses in the range of 50 – 90 μA stimulation (a total of 15 electrodes from 5 slices). Aβ treated slices showed an even smaller excitation. The evoked responses were significantly smaller from 20 μA to 120 μA stimulation intensity (a total of 7 electrodes from 3 slices). Unexpectedly, the slices which were treated with both Zn^{2+} and Aβ showed no evoked responses at any stimulation strength. After recording a 10-min stable control sequence, LTP was induced by TBS (trains of 15×100 Hz bursts, 5 pulses per burst with a 200 ms interburst interval), at the maximum stimulation intensity, fEPSPs were recorded from the distal and proximal part of the stratum radiatum in hippocampal CA1 for 60 min. We weren't able to induce LTP on slices treated with both Zn^{2+} and human Aβ.

5. Discussion

Acute hippocampal slices are widely used in preclinical studies and basic research as a capable experimental model for investigating synaptic structures and functionality at the molecular, cellular, and circuit levels. We developed three novel methods based on the use of acute hippocampal slices and successfully involved these applications into our experiments aimed at exploring and modelling the effects of Aβ aggregation into toxic oligomers – a hallmark in AD – on viability and synaptic functionality of hippocampal tissue.

With the development of *ExViS*, an *ex vivo* universal mini-chamber tube system for acute brain slices, our goal was to be able to study the pathomechanism of various neural disorders and testing drug candidates in a flawless, effective and economic manner. The device is cost-effective to

manufacture and its great advantage compared to other products on the market used for similar tasks is that it is able to keep tissue sections alive in a small media volume for a relative long time (3-4 h). The decreased working volume (max. 1 mL) is particularly useful when very expensive agents are used for treatment. Additionally, a so-called floating incubation is applied, where the slices are less exposed to the distorting effect of gravity, therefore, tissue deformation and flattening do not take place compared to other two-dimensional systems. We have validated the adequacy of our mini-chamber system by testing acute hipocampal slice viability based on the mitochondrial dehydrogenase activity (MTT assay) and the synaptic transmission health by studying TBS induced LTP.

Thanks to this proprietary set up, we were able to design 3-4 h lasting treatments on acute brain slices. To quantify the viability of slices and the effects of different treatments on them, we tailored the MTT assay – widely used in cell lines and primary cell cultures – to suit our *ex vivo* model.

Application of MTT and LDH assays to quantify brain slice viability proved to be an easy *ex vivo* method for studying Aβ1-42 toxicity in brain tissue. Applying an additional OGD pretreatment with Aβ1-42 on hippocampus slices aimed to provide a more relevant *ex vivo* model of the aging brain. The concomitant use of MTT and LDH assays gave reliable results on the toxic effect of Aβ1-42 in OGD acute brain slice model. Both cholorimetric assays are capable of quantifying tissue viability by measuring OD, that is directly proportional with viability in MTT and inversely proportional in LDH assay. The mechanistic explanation behind is that while MTT measures mithocondrial dehydrogenase activity, LDH released to the supernatant medium suggests an increase of tissue and membrane damage. We found that simultaneous application of OGD and Aβ1-42 treatment induced a more intensive decrease in hippocampal slice viability than their separate effects. The method was also successfully validated with classic toxic agents, such as H_2O_2 and Thapsigargin.

During our studies aimed at exploring the effect of Zn^{2+}- induced Aβ1-42 aggregation, we discovered the ability of bis-ANS fluorescent dye, originally used to track low-order oligomers, to label neuronal structures in acute brain tissue. Therefore, we further explored the neuron-labelling properties of the fluorophore and during our studies we found that it only labels mechanically damaged cell membrane in live tissue and it is suitable to label neurite cross-sections on the cutting surface of hippocampal slices. The dye lost this ability if the labelling solution was $NaHCO_3$-free, however the mechanism behind is unknown. Labelled structures could be co-localized with the fluorescent signal of the DNA specific PI on cell level and with intact membrane specific DiI

emission on slice region-level, allowing to obtain detailed imaging of *ex vivo* brain tissue structures. We therefore concluded, that beside its oligomer-specificity, bis-ANS is suitable and easy to use for visualizing the neuronal structures – and to count neurite cross-sections with image analysis methods – on the surface of *ex vivo* brain slices.

Consistent with the literature, we found that the reaction between Zn^{2+} and human Aβ produces toxic Aβ oligomers that form much faster than by spontaneous aggregation. Consequently, LTP and hippocampal viability/mitochondrial activity is inhibited. The mechanism of bis-ANS positive Zn^{2+}-Aβ oligomer toxicity remains uncertain.

We propose an *ex vivo* model for extracellular Aβ aggregation into toxic oligomers that are triggered by endogenous Zn^{2+} release and as a consequence of energy failure with ageing, the tissue does not efficiently reuptake Zn^{2+} released during neurotransmission (Fig. 1). This mechanism leads to increased average extracellular Zn^{2+} promoting Aβ aggregation. Aβ is also released by synaptic activity. Both the Aβ and the Zn^{2+} are trapped into aggregates that initially form close to the synapse and contribute to synaptic dysfunction and aggregates are decomposed after Zn^{2+}-specific chelator is added to the system. The reuptake mechanisms employed to reassimilate Zn^{2+} released in synapses remain to be clarified. Twenty-four zinc transporter proteins are known to date to be specialized to traffic Zn^{2+} into or out of the cytoplasm (e.g. ZnT3 into glutamatergic synaptic vesicles) or out of the cell. There are also known to exist additional ports of uptake into the cell such as the Divalent Metal Transporter 1, AMPA/kainate and NMDA receptors. Zn^{2+} binds to and inhibits the activity of the NMDA receptor and so we hypothesize that the Zn^{2+} intake might reflect internalization through recycling of the NMDA receptor. (The NMDA receptor can mediate some Zn^{2+} uptake, but is not known to be a significant route for Zn^{2+} entry.)

By overcoming some shortfalls of *in vivo* and *in vitro* models, *ex vivo*, acute brain slice technology has been proven to be suitable for studies aiming at exploring molecular events as direct responses to a specific stimulus or treatment affecting viability and function in three dimensional tissue context. The methodology based on acute hippocampal slices developed in our laboratory to measure Aβ1-42 oligomer toxicity provides relevant and cost-effective model for screening protective agents and test hypothesis in pre-clinical studies in relatively short time frame. It allows iterative testing, tissue-level toxicology as well as detailed and easy imaging.

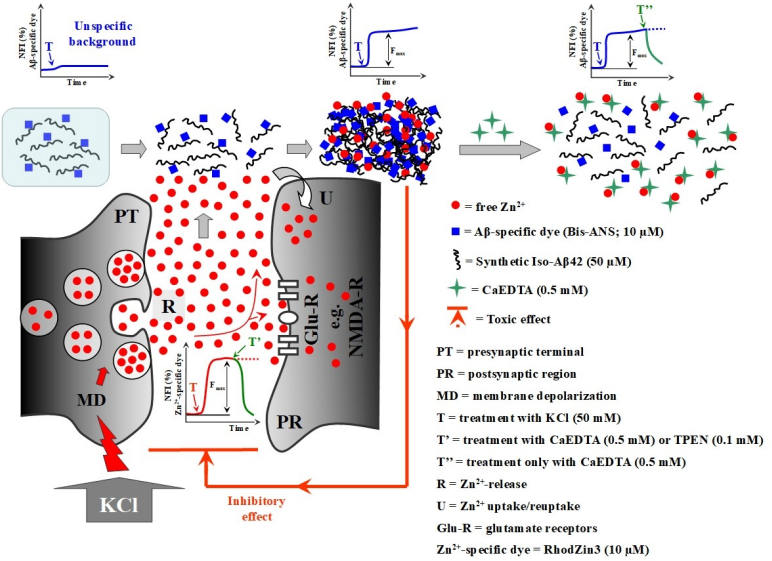

Figure 1: Schematic representation of Zn^{2+}-release induced Aβ aggregation in the synaptic cleft and its effect on hippocampal synaptic functionality

6. Conclusion

To overcome the shortcomings of the *in vitro* and *in vivo* methods, we developed a cost effective and simple apparatus for maintaining the viability of acute tissue slices, named: *ExViS* (*Ex Vivo* System; Universal Mini-Chamber Tube System for Acute Tissue Slices). The system allowed us to further develop methods that use acute (*ex vivo*) hippocampal slices to model AD-related patomechanisms. Over the course of my PhD studies we have developed the following techniques and *ex vivo* models based on the features of acute hippocampal slices:

1. Rapid, reliable and quantitative determination of Aβ1-42 toxicity in ageing (OGD) acute hippocampal slice model using MTT and LDH assays.
2. Quantitative determination of Zn^{2+}-induced Aβ1-42 oligomerization toxicity in acute hippocampal slice model using MTT assay.

3. Fluorescent imaging of neurite cross-sections and detailed imaging of neurite structures in acute hippocampal slices via a novel application of bis-ANS and its co-staining variations.
4. Modelling the effect of Zn^{2+} released in glutamergic synaptic cleft in the hippocampus on Aβ1-42 aggregation and its consequences on cell viability and synaptic functionality, learning and memory (LTP).

The acute hippocampus slice-based models can serve as a feasible tool to gain deeper understanding on how pathological events in AD, in particular Aβ oligomerization, influence hippocampal functionality and therefore paving the way to develop and test related hypothesis but also to screen potential protective agents or validate results seen *in vivo* or predicted *in silico.*

7. Aknowledgement

I would like to thank the following people, without whom I would not have been able to complete this research, and without whom I would not have made it through my PhD degree. My Supervisor and friend **Dr. Zsolt Datki**, whose expertise and knowledge of the subject matter steered me through this research. He supported me both professionally and as a human being in challenging times and created a new opportunity for me to re-uptake the thread of a research we had started a while ago. I am especially grateful to **Prof. Dr. Botond Penke**, who offered many opportunities to evolve professionally and was a role model of dedicated scientist for me. To **Dr. Ákos Hunya**, who introduced me into the main skills and techniques necessary to become a useful member of our lab team. To **Dr. Lívia Fülöp** and **Dr. Zsolt Bozsó** for their expert support in biochemistry and to **Dr. Viktor Szegedi** for his expertise and for making the electrophysiological studies possible. To **Dr. Zita Galik-Oláh** for offering her time and patience to thoroughly review this dissertation. To **Mónika Országné Mihók** and **Mária Batki** who are the most amazing laboratory technicians I've ever met, for their patience and expert support, that made all procedures flawless, as well as for their friendship and all the fun moments we've had together.

As the mother of a wonderful but demanding toddler, I wouldn't been able to find uninterrupted time to write this thesis and to pass my exam, without the dedication of **my husband** (who also helped me with editing the figures of this thesis) **and my family** who created a peaceful environment and supported and encouraged me along the way.